

Enhancement of Infrared-Emitting Quantum Dots Photoluminescence Via Plasmonic Nanoarrays

A. A. Sergeev^{a,*} (ORCID: 0000-0002-8294-865X), K. A. Sergeeva^a, D. V. Pavlov^{a,b}, and A. A. Kuchmizhak^{a,b}

^a Institute of Automation and Control Processes, Far Eastern Branch, Russian Academy of Sciences, Vladivostok, 690041 Russia

^b Far Eastern Federal University, Vladivostok, 690950 Russia

* e-mail: sergeev@iacp.dvo.ru

Received September 20, 2022; revised October 14, 2022; accepted October 20, 2022

Abstract—Control over the radiative and non-radiative channels of the IR-emitting quantum dots (QDs) is crucially important to improve performance of related devices. Here, we study spontaneous photoluminescence (PL) enhancement of mercury telluride QDs coupled to plasmonic nanoantenna arrays supporting collective plasmon mode spectrally matching QD's PL spectrum. Our systematic studies revealed how PL enhancement varies with QDs layer thicknesses as well as laser excitation and emission collection conditions, providing deeper insight into the QD/plasmonic arrays interaction. We demonstrated that careful adjustment of excitation and emission collection parameters leads to more than an order of magnitude enhancement of spontaneous emission of HgTe QDs coupled with periodical plasmonic arrays with resonances spectrally matched to QDs absorption and emission bands. The region of QDs layer thickness, wherein plasmon-related quenching and dot-to-dot resonance energy transfer have the minimal impact and, hence the PL enhancement has the maximal factor, had been determined.

Keywords: IR-resonant nanostructures, nanostructure arrays, infrared photonics, quantum dots, luminescence enhancement

DOI: 10.3103/S106287382270068X

INTRODUCTION

To date, near-infrared emitting quantum dots (QDs), namely mercury telluride (HgTe), are considered the most promising candidate for developing novel light-emitting and photodetecting devices covering range from short- to long-waves [1]. Along with the typical processes negatively affecting QD-based device performance in general (for example, Auger recombination, as well as structural and surface defects), infrared QDs have a number of additional factors limiting their functional properties. First, there is a fundamental limitation that follows from Fermi's Golden Rule and links a decrease in the radiative recombination rate with a decrease of the quantum emission frequency (or transition frequency in general). Moreover, vibrations of molecules or functional groups of organic ligands, that are frequently used to stabilize QDs and are inevitably present on their surface, introduce additional absorption dips into the luminescence spectrum and act as nonradiative charge carrier recombination centers due to the formation of a polaron (a quasiparticle formed by an exciton and a localized phonon). Despite that the theory of exciton-phonon interaction provides for the possible energy exchange between these quasiparticles [2], which also

implies the possibility for radiative recombination, there is no experimental confirmation of this process. Thus, this quasiparticle interaction is considered only as an additional channel of nonradiative relaxation of the excitation energy. The energy transferred to the polaron's optical frequency (e.g. LO) vibrational transitions may then couple down to acoustic frequency phonons and then be dissipated as the ligands interact by collisions with surrounding materials.

As to the practical performance of nanomaterials based on heavy metal chalcogenide QDs, it is extremely important to obtain homogeneous conductive coatings using a simple and efficient method of their formation from a solution (spin-coating, immersion, drop-casting, etc.). However, recent methods for the synthesis of QDs, which provide a smooth change in their absorption and emission spectra, are generally conducted with long-molecular ligands to stabilize what are often relatively large particles [3]. The inorganic core of the QDs can range from 3–10 nm diameter for NIR/SWIR materials, up to a few tens of nm sizes for mid-wave IR and long-wave IR applications. In this case, obtained QD coatings have low conductivity and require a ligand exchange procedure (replacing the long alkyl chain ligands with shorter or ionic ligands), which usually undermines the film morphol-

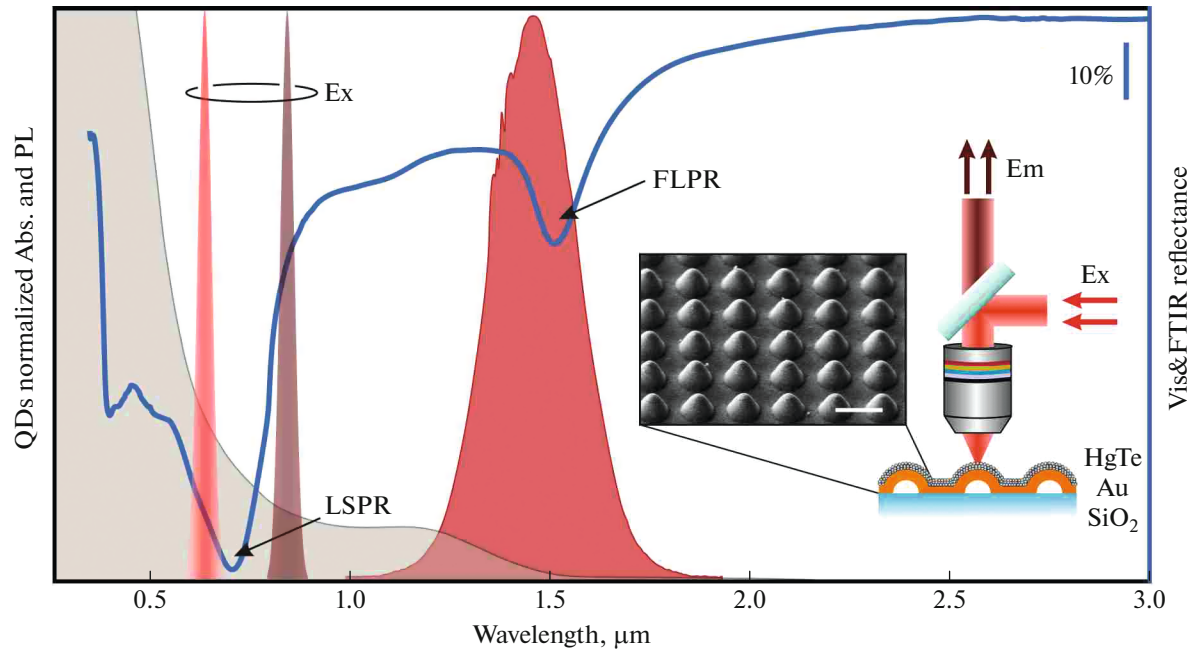


Fig. 1. Absorption/photoluminescence (gray and red shaded) spectra of HgTe QDs as well as reflection spectra (blue curve) of plasmonic structures used in this study. HgTe QDs spectra were normalized at the maximum value within a given spectral range. The scheme of the experiment is shown in the inset.

ogy and leads to the appearance of additional centers of nonradiative recombination.

Previously [4], we have shown that most of these factors can be overcome through combining QDs with plasmonic structures having the resonances spectrally matching with the excitation or emission bands of a QD, leading to noticeable QDs photoluminescence (PL) enhancement. Nevertheless, some factors affecting PL enhancement via resonant plasmonic nanoarrays are still remains unclear. First of all, it is the role of collective plasmon resonances and resonances of a single nanostructure in overall PL enhancement. Then, the enhancement efficiency at consistently increasing thickness of the QDs layer needs to be tracked. Finally, the evaluation of angular dependence of excitation and collection conditions may open a way toward deeper understanding of the enhancement processes. In this work, we consequently studied these issues and distinguished their contributions to the tailoring of the emission properties of mercury telluride quantum dots

EXPERIMENT AND AVAILABLE SOUND SPEED MEASUREMENT DATA

The details for plasmonic metasurfaces fabrication and quantum dots synthesis can be found elsewhere [3, 4]. Briefly, the plasmonic structures were fabricated through direct ablation-free laser nanopatterning of 50 nm-thick gold film on a glass substrate. Once laser pulse shoots gold film, it locally melts and, fol-

lowing processes of dewetting and resolidification, results in bump-like structure formation, which is partially de-attached from the substrate keeping at the same time the film consistency (inset in Fig. 1). The ordered arrays of nanobumps demonstrate complex resonance spectra formed by first-order lattice plasmon resonance (FLPR) in the infra-red region and a superposition of high-order lattice plasmon resonances (HLPR) and localized plasmon resonances (LSPR) of isolated nanobumps in the visible range (blue curve in Fig. 1). The FLPR position depends on the nanobump' size and array' period, while visible-range resonances mostly keep in the same spectral range, probably due to the abovementioned complicated nature. It should be noted that due to the strong overlap between LSPR and HLPR peaks their exact position can't be distinguished.

HgTe QDs were synthesized via selective-grow cold injection technique allowing precise control of QDs size and, correspondingly, the PL spectral maximum via synthesis temperature and its duration. As a result, a batch of HgTe QDs with emission spectrally overlapping with FLPR was obtained (Fig. 1).

To track the PL enhancing phenomena evolution with QDs layer thickness, the as-prepared solution was diluted down to 1011 dots/mL and deposited on spinning at 1000 rpm substrate. Before first layer deposition, the substrate was rinsed with dodecanethiol (the QDs ligand) to increase the QDs adhesion. All further layers, 10 in total, were deposited without dodecanethiol rinsing. The dependence of film thick-

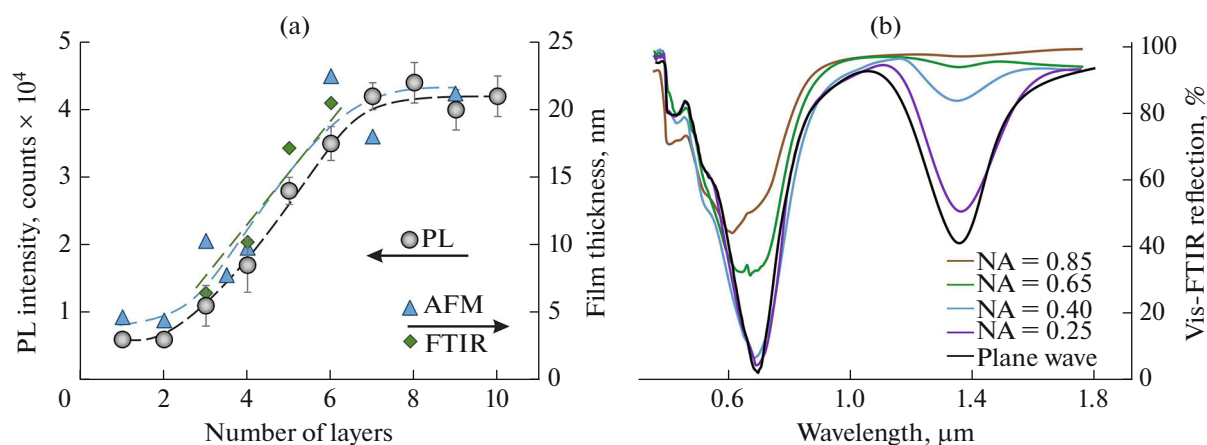


Fig. 2. (a) The dependence of QDs film thickness on the number of spin-coated layers measured by various techniques. (b) The reflection spectra of nanobumps arrays measured at different NAs.

ness on the number of deposited layers was determined by a combination of atomic-force microscopy, Fourier infrared transform, and photoluminescent spectroscopies, as will be described later.

The experimental studies were carried out on F900 (Edinburgh Instruments) spectrometer combined with a home-built micro-PL setup. To estimate the impact of excitation from plasmon resonances in the visible range the solid-state lasers emitting at 685 and 880 nm were used as excitation sources (shaded peaks in Fig. 1). Newport M-series microscope lenses with NAs ranging from 0.1 to 0.85 were used for excitation and emission collection.

SAMPLE PREPARATION AND CHARACTERISATION

Layer-by-layer deposition leads to the nonlinear increase of the QDs film thickness (Fig 2a). According to AFM data, two deposited layers have an average thickness of around 4 ± 1 nm, corresponding to monolayer-thick QDs film. Probably, after the first depositing cycle, the film is non-uniform and doesn't cover the entire sample surface. Deposition of subsequent layers results in a gradual increase of film thickness up to the seventh deposited layer. After that, deposition of additional layers leads to no increase in film thickness, caused by partial dissolution of the film during QDs solution casting followed by re-deposition of QDs from the casted solution. The PL from the smooth gold film (further used as a reference in PL enhancement studies) follows the same trend with the film thickness, indicating the absence of any noticeable quenching effects due to close QDs spacing. The limitation on the QDs film thickness can be overcome using a more concentrated stock solution. However, in that case, it is hard to deposit monolayer-thick film, even at a reasonably high (3000 rpm) spin-coating

speed. In this regard, the only way for the film thickness to increase is a drop-casting.

Drop-casted films are less uniform than spin-coated ones, but their thickness could reach 100 nm and even higher. By applying QDs over plasmonic nanostructures, the FLPR position linearly redshifts to 2 nm per each 1 nm of the deposited QD layer [5]. Linear dependence preserved up to 100-nm thick layer. For thicker layers, the FLPR broadens (starting from 20 nm-thick layers), complicating the detection of its spectral position.

PL ENHANCEMENT STUDIES

Owing to strong angular dispersion [6], the collective plasmon resonances Q-factor (e.g., the ratio of full width at half maximum of the reflection dip and the corresponding wavelength at the dip minimum) depends on the range of incident angles of the pump radiation, that is defined by the NA of the focusing lens (Fig. 2b). Noteworthy, the highest Q-factor (≈ 10) of as-prepared nanobumps array FLPR was achieved upon measuring the reflection spectra with low-NA optics (NA = 0.25), followed by its broadening and decreasing in intensity with NA increasing. At excitation with NA = 0.85, the FLPR becomes almost indistinguishable from the reflection spectra of the smooth gold film.

A few monolayer-thick QD film (below 7 nm) demonstrate a distinct from reference area absolute PL intensity dependence on NA. Whilst PL intensity from the reference area gradually increases with increasing NA, the film on the nanobumps shows a maximal PL at NA = 0.65 (Fig. 3). In a case of $\lambda_{\text{EX}} = 685$ nm, that is the only NA, wherein a monolayer-thick QDs film shows PL intensity compatible to those measured from the reference area. The PL intensity from a single deposited layer measured at other NAs is much lower than the reference one. This feature indi-

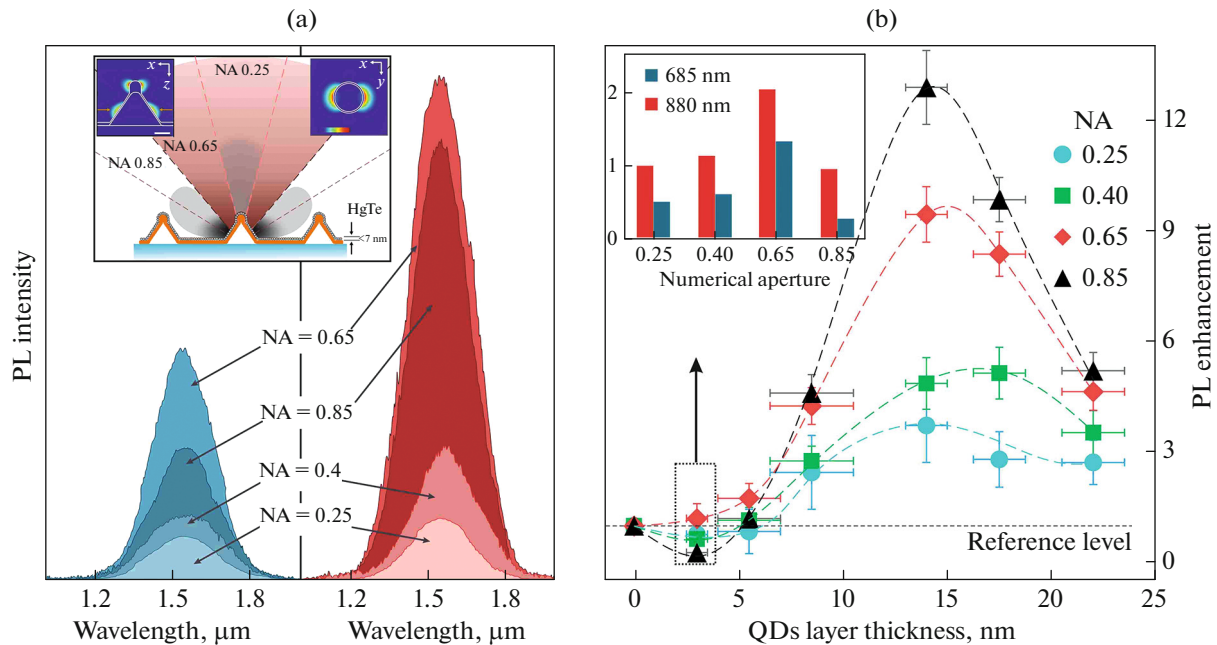


Fig. 3. (a) Absolute PL intensity measured at different NA from monolayer-thick QDs film at excitation close to LSPR (685 nm, left) and apart from it (880 nm, right). Inset shows FDTD calculated EM-field intensity distribution near the isolated nanobump, as well as collection angles for various NAs. (b) PL enhancement factor versus the QDs layer thickness measured for various NAs of the focusing lens used for excitation and emission collection. Inset shows the PL enhancement from monolayer-thick QDs film at 685 and 880 nm excitation.

causes plasmon-mediated quenching of the quantum emitter's PL via non-radiative decay in the vicinity of the metallic surface. According to FDTD simulations (inset in Fig. 3a), nanobumps have two hotspot areas: on the top of the nanostructure and in the middle of its sides. The position of these hotspots matches well with the collection angles on NA = 0.25 and NA = 0.85 demonstrating the maximal PL quenching in a case of monolayer-thick QD film (inset in Fig. 3b). Moreover, at $\lambda_{\text{EX}} = 880$ nm the general trend of absolute PL intensity dependence on NA remains almost the same (with the maximum at NA = 0.65), and its amplitude becomes compatible or even higher than from reference area. Taking into account that $\lambda_{\text{EX}} = 880$ nm is reasonably far from the LSPR position, one can suggest that in the case of monolayer-thick film detected PL increase originates from competition between near-field quenching on LSPR and enhancement due to PL coupling with the FLPR.

Further increase of the layer thickness leads to a sharp increase of PL enhancement factor to ≈ 13 achieved for 12 nm thick layer thickness at NA = 0.85. Noteworthy, for the lowest tested NA = 0.25 maximal, 5-fold, PL enhancement occurs for 18 nm thick QDs layer. Systematic measurements performed for intermediate NA values give the maximal PL enhancement achieved for QD layer with the thickness ≈ 12 –15 nm.

The absence of PL enhancement for thin QD layers highlights the existence of quenching processes

through intrinsic plasmonic losses, which probably decays in a range up to 10 nm layer thickness (2–4 QD monolayers), wherein excitation with any NA leads to PL enhancement. The results also highlight that QDs capping smooth Au film emit light predominantly in a vertical direction, resulting in the absence of the PL enhancement dependence versus collection angle, in sharp contrast to the QDs on the plasmonic nanostructure array.

Combining the results obtained, one can conclude that achieving the maximal PL enhancement requires the reduction of non-radiative channels, both plasmonic and QDs intrinsic nature. In this regard, the only way to fulfill these issues is to use a thin, up to 20 nm QDs layer separated from plasmonic structures with a spacer layer no less than 6-nm thickness.

CONCLUSIONS

We demonstrated that careful adjustment of excitation and emission collection parameters leads to more than an order of magnitude enhancement of spontaneous emission of HgTe QDs coupled with periodical plasmonic arrays with resonances spectrally matched to QDs absorption and emission bands. The region of QDs layer thickness, wherein plasmon-related quenching and dot-to-dot resonance energy transfer have the minimal impact and, hence the PL enhancement has the maximal factor, had been determined.

FUNDING

The financial support from the Russian Science Foundation (project no. 21-79-10197) is gratefully acknowledged.

CONFLICT OF INTEREST

The authors declare that they have no conflicts of interest.

REFERENCES

1. Greboval, C., Chu, A., Goubet, N., Livache, C., Ithurria, S., and Lhuillier, E., *Chem. Rev.*, 2021, vol. 121, no. 7, p. 3627.
<https://doi.org/10.1021/acs.chemrev.0c01120>
2. Burdov, V.A. and Vasilevskiy, M.I., *Appl. Sci.*, 2021, vol. 11, no. 2, 497.
<https://doi.org/10.3390/app11020497>
3. Kershaw, S.V., Yiu, W.K., Sergeev, A., and Rogach, A.L., *Chem. Mater.*, 2020, vol. 32, no. 9, p. 3930.
<https://doi.org/10.1021/acs.chemmater.0c00249>
4. Sergeev, A.A., Pavlov, D.V., Kuchmizhak, A.A., Lapine, M.V., Yiu, W.K., Dong, Y., Juodkazis, S., Zhao, N., Kershaw, S.V., and Rogach, A.L., *Light: Sci. Appl.*, 2020, vol. 9, no. 1, 16.
<https://doi.org/10.1038/s41377-020-0247-6>
5. Pavlov, D.V., Zhizhchenko, A.Yu., Honda, M., Yamana-ka, M., Vitrik, O.B., Kulinich, S.A., Juodkazis, S., Kudryashov, S.I., and Kuchmizhak, A.A., *Nanomaterials*, 2019, vol. 9, 1348.
<https://doi.org/10.3390/nano9101348>
6. V. Kravets, G., Kabashin, A.V., Barnes, W.L., and Grigorenko, A.N., *Chem. Rev.*, 2018, vol. 118, p. 5912.
<https://doi.org/10.1021/acs.chemrev.8b00243>